



## Technical Note

# An experimental study of the airside performance of the superslit fin-and-tube heat exchangers

Yuan-Jan Du<sup>a</sup>, Chi-Chuan Wang<sup>b,\*</sup><sup>a</sup>*Energy & Resources Laboratories, Industrial Technology Research Institute, Hsinchu 310, Taiwan*<sup>b</sup>*D500 ERL/ITRI, Bldg. 64, 195~6 Section 4, Chung Hsing Road, Chutung, Hsinchu, Taiwan*

Received 2 August 1999; received in revised form 28 February 2000

## 1. Introduction

Interrupted surfaces are often employed in plate-finned heat exchangers to effectively improve the heat transfer performance. Interrupted surfaces were often in the form of louver or slit (lance). For practical implementation of the air-cooled heat exchangers, the interrupted fin patterns are often accompanying with round tube, hence, periodic expansion/contraction of airflow within the heat exchangers are encountered. Therefore, the airflow pattern within interrupted surfaces is very complex owing to the presence of the round tube. There had been many researches devoted to the study of interrupted surfaces like slit fin geometry [1–4]. However, these studies were normally focused on the fundamental understanding of the slit fin surfaces. Experimental data in association with the actual performance of the fin-and-tube heat exchangers having slit fin geometry were very rare.

The only papers related to this subject were by Nakayama and Xu [5] and Wang et al. [6]. Nakayama and Xu [5] presented test results for three samples, and proposed a correlation based on their test results. However, as pointed out by Garimella et al. [7], applicability of the correlation by Nakayama and Xu [5] is very limited. Extrapolation of the correlations is inadvisable due to the very strong dependence of the  $j$ -fac-

tor on the ratio of fin thickness to fin spacing. In a recent study, Wang et al. [6] provide test results for a conventional slit fin geometry. Their results indicated that the heat transfer performance increase with decrease of fin pitch for  $N = 1$ . However, for  $N \geq 4$ , the effect of fin pitch on the heat transfer performance is reversed.

The purpose of the present study is thus twofold. Firstly, further experimental data are provided to understand the details of the slit fin geometry. Secondly, based on the test (newly test results) and those reported by Nakayama and Xu [5], and Wang et al. [6], an updated airside that can cover a much wider applicable range correlation is proposed.

## 2. Experimental apparatus and reduction methods

In this study, a total of 31 samples of fin-and-tube heat exchangers having slit geometry were investigated in the present study. Their related geometric parameters are tabulated in Table 1. Detailed dimensions of the slit fin patterns are illustrated in Fig. 1. As seen in the figure, two types of superslit fin geometry were examined (type I and type II). For comparison purpose, previous tested slit fin geometry by Wang et al. [6] was also shown in Fig. 1C. Note that Fig. 1C is the conventional slit geometry with one-side interrupted surface. The present superslit fin possesses an offset slit geometry. Detailed definitions of the slit fin geometry can be seen in Fig. 1D.

For the sake of simplicity, detailed description of

\* Corresponding author. Tel.: +886-3-591-6294; fax: +886-3-582-0250.

E-mail address: ccwang@itri.org.tw (C.-C. Wang).

### Nomenclature

$A_o$	total surface area (m <sup>2</sup> )	$Nu$	Nusselt number, dimensionless
$D_c$	fin collar outside diameter (mm)	$P_l$	longitudinal tube pitch (mm)
$f$	friction factor, dimensionless	$P_t$	transverse tube pitch (mm)
$f_1, f_2, f_3$	correlation parameter	$Re_{D_c}$	Reynolds number based on tube collar diameter, $G_c D_c / \mu_{air}$ , dimensionless
$F_p$	fin pitch (mm)	$Pr$	Prandtl number, dimensionless
$F_s$	fin spacing (mm)	$S_h$	height of slit (mm)
$j$	$Nu / Re Pr^{1/3}$ , the Colburn factor, dimensionless	$S_s$	breadth of a slit in the direction of air-flow (mm)
$j_1, j_2, j_3, j_4$	correlation parameter	$S_w$	width of slit (mm)
$S_n$	number of slits in an enhanced zone, dimensionless	$\delta_f$	fin thickness (m)
$N$	number of longitudinal tube rows, dimensionless	$\mu_{air}$	air viscosity (N s m <sup>-2</sup> )

the test facility and the related reduction method of the heat transfer performance are omitted, one can find the associated details from previous investigation [6]. Tests were performed in fully dry test conditions. Uncertainties of the Colburn  $j$  factor and friction factor  $f$  were estimated by the method suggested by Mofat [8]. The uncertainties ranged from 2.4 to 14.1% for the  $j$  factors, and 3.1 to 17.9% for  $f$ . The highest uncertainties were associated with lowest Reynolds number.

### 3. Results and discussion

Fig. 2 shows the test results for type I superslit geometry with  $N = 1$ . The fin pitches are from 1.5 to 2.5 mm. The ordinates are  $j$  and  $f$  while the abscissa is the Reynolds number based on collar diameter. As seen in the figure, the heat transfer performance for the type I slit fin geometry can be roughly classified into two group. The heat transfer performance for  $F_p \leq 2.1$  mm is about 20–25% higher than those of  $F_p > 2.1$  mm. The results are different from those of the slit fin geometry by Wang et al. [6] and those of the louver fin reported by Wang et al. [9]. For louver fin and  $N = 1$ , as shown by Wang et al. [9], the effect of fin spacing on the heat transfer performance is relatively small ( $F_p = 1.2$ – $2.5$  mm). For conventional slit fin geometry (Fig. 1C), Wang et al. [6] reported that the heat transfer performance gradually increased from dense fin spacing to sparse fin spacing ( $F_p = 1.2$ – $2.5$  mm). For type II superslit geometry of  $N = 1$  as seen in Fig. 3, the results are analogous to those reported by Wang et al. [6]. In seeking connection of this phenomenon, it is necessary to examine the detailed fin geometry of the type I superslit fin. A close examination of the type I geometry indicated that the slit was not par-

allel. A slight chevron is observed for type I geometry which is similar to a convex strip to some extent.

For a particular fin pitch and wave height of convex-louver strip, Pauley and Hodgson [10] reported that the mixing angle usually increased with the Reynolds number. It is noticed that the mixing angle was defined as the inclined angle formed by the dye, as measured from the louver of first contact. Pauley and Hodgson [10] reported that the mixing angle was related to the parameter,  $F_p / 4H$ . Where  $H$  is the height of louver. They found that, for  $F_p / 4H = 3$ , the mixing angle decreases with the increase of the Reynolds number. Based on their flow visualization experiments, Pauley and Hodgson [10] argued that an inviscid Rayleigh instability may cause the unsteadiness of the shear layer for  $F_p / 4H$  near 3. The velocity difference across the shear layer was large enough to cause vortex rollup, and the mixing region was contained primarily within the louvers and did not extend between the fin rows. Therefore, a decrease of mixing angle, and lower heat transfer performance is shown when the fin pitch is decreased to a certain value. The present  $F_p / 4H$  values are approximately 1.78 ( $F_p = 1.5$  mm), 2.26 ( $F_p = 1.9$  mm), and 2.98 ( $F_p = 2.5$  mm). Therefore, for the present type I geometry, it is very likely that when the fin pitch is above certain value, the mixing angle may decrease with the Reynolds number and result in the degradation of heat transfer performance. The results imply the detectable difference of the type I slit fin geometry may be related to different type enhanced mechanism. Instability caused by the vortex shedding is less profound as  $F_p$  is increased over 2.1 mm.

Figs. 4 and 5 illustrate the effect of the number of tube rows on the heat transfer and friction characteristics for the present superslit geometry. The fin pitches are 1.5 and 2.5 mm for type I and 1.2 and 1.6 mm for

Table 1  
Geometric dimensions of the slit fin-and-tube heat exchangers

No.	References	$F_p$ (mm)	$D_c$ (mm)	$P_t$ (mm)	$P_l$ (mm)	$\delta_r$ (mm)	$N$	No. of $j$ data	No. of $f$ data
1	This study, type I	1.48	10.32	21.65	25	0.11	1	10	10
2	This study, type I	1.71	10.32	21.65	25	0.11	1	9	9
3	This study, type I	1.88	10.32	21.65	25	0.11	1	9	9
4	This study, type I	2.10	10.32	21.65	25	0.11	1	9	9
5	This study, type I	2.24	10.32	21.65	25	0.11	1	10	10
6	This study, type I	2.50	10.32	21.65	25	0.11	1	10	10
7	This study, type I	1.51	10.32	21.65	25	0.11	2	10	10
8	This study, type I	1.71	10.32	21.65	25	0.11	2	10	10
9	This study, type I	1.87	10.32	21.65	25	0.11	2	10	10
10	This study, type I	2.11	10.32	21.65	25	0.11	2	10	10
11	This study, type I	2.30	10.32	21.65	25	0.11	2	10	10
12	This study, type I	2.50	10.32	21.65	25	0.11	2	10	10
13	This study, type I	1.51	10.32	21.65	25	0.11	3	10	10
14	This study, type I	1.70	10.32	21.65	25	0.11	3	10	10
15	This study, type I	1.88	10.32	21.65	25	0.11	3	10	10
16	This study, type I	2.10	10.32	21.65	25	0.11	3	10	10
17	This study, type I	2.50	10.32	21.65	25	0.11	3	10	10
18	This study, type I	1.51	10.32	21.65	25	0.11	4	10	10
19	This study, type I	1.70	10.32	21.65	25	0.11	4	9	9
20	This study, type I	1.92	10.32	21.65	25	0.11	4	10	10
21	This study, type I	2.10	10.32	21.65	25	0.11	4	10	10
22	This study, type I	2.50	10.32	21.65	25	0.11	4	9	9
23	This study, type II	1.20	7.52	17.32	20	0.11	1	11	11
24	This study, type II	1.40	7.52	17.32	20	0.11	1	11	11
25	This study, type II	1.60	7.52	17.32	20	0.11	1	11	11
26	This study, type II	1.20	7.52	17.32	20	0.11	2	11	11
27	This study, type II	1.40	7.52	17.32	20	0.11	2	11	11
28	This study, type II	1.60	7.52	17.32	20	0.11	2	11	11
29	This study, type II	1.20	7.52	17.32	20	0.11	3	10	10
30	This study, type II	1.40	7.52	17.32	20	0.11	3	11	11
31	This study, type II	1.60	7.52	17.32	20	0.11	3	11	11
32	Wang et al. [6]	1.28	10.34	25.4	22	0.12	1	10	10
33	Wang et al. [6]	1.76	10.34	25.4	22	0.12	1	10	10
34	Wang et al. [6]	2.43	10.34	25.4	22	0.12	1	10	10
35	Wang et al. [6]	1.21	10.34	25.4	22	0.12	2	10	10
36	Wang et al. [6]	1.79	10.34	25.4	22	0.12	2	10	10
37	Wang et al. [6]	2.46	10.34	25.4	22	0.12	2	10	10
38	Wang et al. [6]	1.22	10.34	25.4	22	0.12	4	10	10
39	Wang et al. [6]	1.22	10.34	25.4	22	0.12	4	10	10

(continued on next page)

Table 1 (continued)

No.	References	$F_p$ (mm)	$D_c$ (mm)	$P_t$ (mm)	$P_1$ (mm)	$\delta_r$ (mm)	$N$	No. of $j$ data	No. of $f$ data
40	Wang et al. [6]	2.47	10.34	25.4	22	0.12	4	11	11
41	Wang et al. [6]	1.21	10.34	25.4	22	0.12	6	9	9
42	Wang et al. [6]	1.78	10.34	25.4	22	0.12	6	10	10
43	Wang et al. [6]	2.48	10.34	25.4	22	0.12	6	10	10
44	Nakayama and Xu [5]	2.00	16.30	38	33	0.15	2	0	7
45	Nakayama and Xu [5]	1.70	16.30	38	33	0.15	2	0	5
46	Nakayama and Xu [5]	2.50	16.30	38	33	0.15	2	0	4
47	Nakayama and Xu [5]	2.50	16.4	38	33	0.18	2	12	0
48	Nakayama and Xu [5]	1.90	9.90	25	22	0.2	2	0	7
49	Nakayama and Xu [5]	2.50	9.90	25	22	0.2	2	0	10
50	Nakayama and Xu [5]	2.00	8.4	28	15	0.2	6	4	0
Number of data used to develop correlation								449	466

type II geometry, respectively. The effect of the number of tube row on the friction factors are relatively small. Basic heat transfer characteristics of the present fin geometry in conjunction with the effect of the tube row are summarized as follows:

1. For  $Re_{D_c} < 2000$ , higher heat transfer performance is seen for  $N = 1$  in comparison with multiple number of tube row. However, one can see that the characteristics are reversed when  $Re_{D_c} > 2000$ . The heat transfer performance for  $N = 1$  is lower than those of having multiple rows and the difference increases with increase of the Reynolds number. Apparently this is due to the additional vortex shedding caused by the blockage of the tube row.
2. For dense fin pitches like  $F_p = 1.2$  or  $1.5$  mm at  $Re_{D_c} < 1000$ , the heat transfer performance drops very sharply with the number of tube row. The results can be interpreted from the observations by Mochizuki et al. [11]. For offset slit geometry at low Reynolds number region, they found that steady laminar flow patterns prevailed throughout the core. This implies that the heat transfer performances may deteriorate significantly as the depth of the core is increased.
3. For multiple row configuration, the effect of the number of tube row is very small when  $Re_{D_c} > 2000$ . Observations of Figs. 4 and 5 reveal that the effect of tube row for type II is almost negligible. Again, this phenomenon can be explained from those observations by Mochizuki et al. [11]. They reported that as the Reynolds number reached a significantly high value, the turbulent intensity became nearly uniform throughout the core. This phenomenon is especially pronounced for offset slit fin geometry having smaller fin length.

From the previous discussions, the airside performances of the present slit fin are very complicated. Furthermore, a detectable “level-off” phenomenon for the heat transfer performance is observed for dense fin pitch for  $N > 2$ . Therefore, we had conducted a multiple regression to correlate the test results. Test results for a total of 50 samples of fin-and-tube heat exchangers are used to develop the correlation (see details in Table 1). The data bank includes those from this study (31 samples, Fig. 1A and B), Wang et al. [6] (12 samples, Fig. 1C), and Nakayama and Xu [5] (7 samples, Fig. 1C). The proposed correlations are given as follows:

$$j = 5.98 Re_{D_c}^{j_1} \left(\frac{F_s}{D_c}\right)^{j_2} N^{j_3} \left(\frac{S_w}{S_h}\right)^{j_4} \left(\frac{P_t}{P_1}\right)^{0.804} \quad (1)$$

$$f = 0.1851 Re_{D_c}^{f_1} \left(\frac{F_s}{D_c}\right)^{f_2} \left(\frac{S_w}{S_h}\right)^{f_3} N^{-0.046} \quad (2)$$

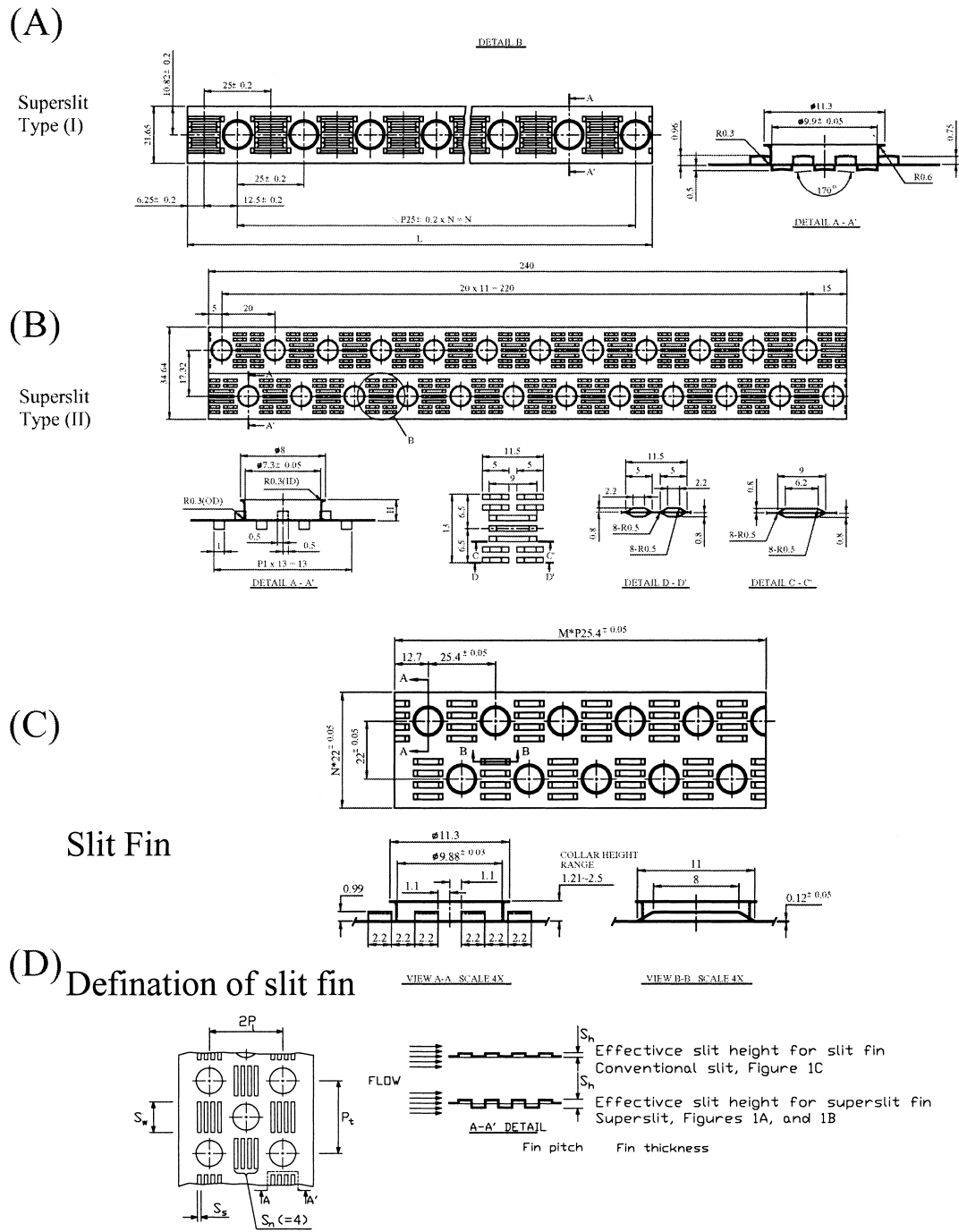


Fig. 1. Schematic of the terminology of the slit fin geometry.

where

$$j_1 = -0.647 + 0.198 \frac{N}{\log_e(Re_{D_c})} - 0.458 \frac{F_s}{D_c} + 2.52 \frac{N}{Re_{D_c}} \quad (3)$$

$$j_2 = 0.116 + 1.125 \frac{N}{\log_e(Re_{D_c})} + 47.6 \frac{N}{Re_{D_c}} \quad (4)$$

$$j_3 = 0.49 + 175 \frac{F_s/D_c}{Re_{D_c}} - \frac{3.08}{\log_e(Re_{D_c})} \quad (5)$$

$$j_4 = -0.63 + 0.086 S_n \quad (6)$$

$$f_1 = -1.485 + 0.656 \left( \frac{F_s}{D_c} \right) + 0.855 \left( \frac{P_1}{P_2} \right) \quad (7)$$

$$f_2 = -1.04 - \frac{125}{Re_{D_c}} \quad (8)$$

$$f_3 = -0.83 + 0.117 S_n \quad (9)$$

Thus, Eq. (1) can describe 92.2 of the  $j$  factors within 15% while Eq. (2) can correlate 94.6% of the friction factors within 15%. The mean deviation of Eq. (1) is 8.04% and for Eq. (2) is 5.44%.

#### 4. Conclusions

Experimental study on the airside performances of fin-and-tube heat exchangers having slit fin geometry was carried out. Major conclusions of this study is summarized as follows:

- For  $N = 1$ , the heat transfer performance of slit fin-and-tube heat exchangers increase with decrease of fin pitch. However, for  $N > 2$ , the effect of fin pitch on the heat transfer performance is reversed.
- For  $Re_{D_c} < 1000$ , the heat transfer performance decreases significantly with the number of tube row.
- For  $Re_{D_c} > 2000$ , the heat transfer performance is relatively insensitive to change with the number of tube row. The effect of the number of tube row is almost negligible for smaller slit length (like type II

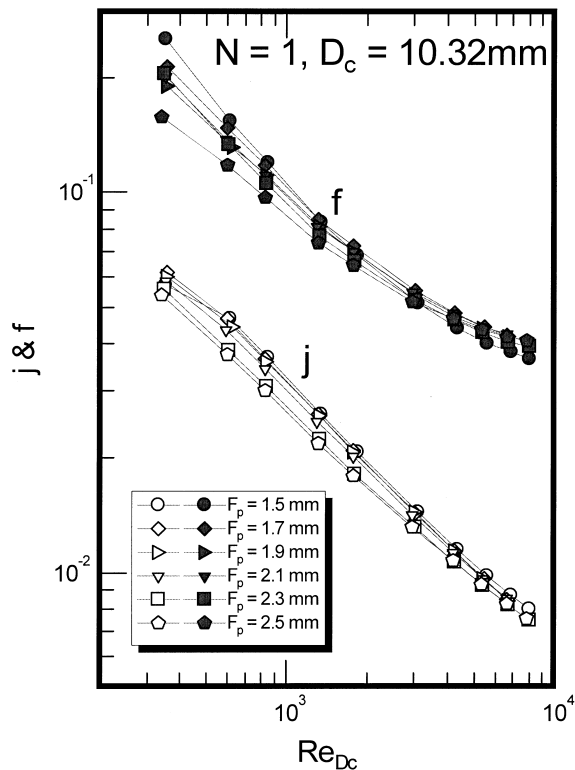


Fig. 2. Effect of fin pitch on the air side performance for type I fin geometry and  $N = 1$ .

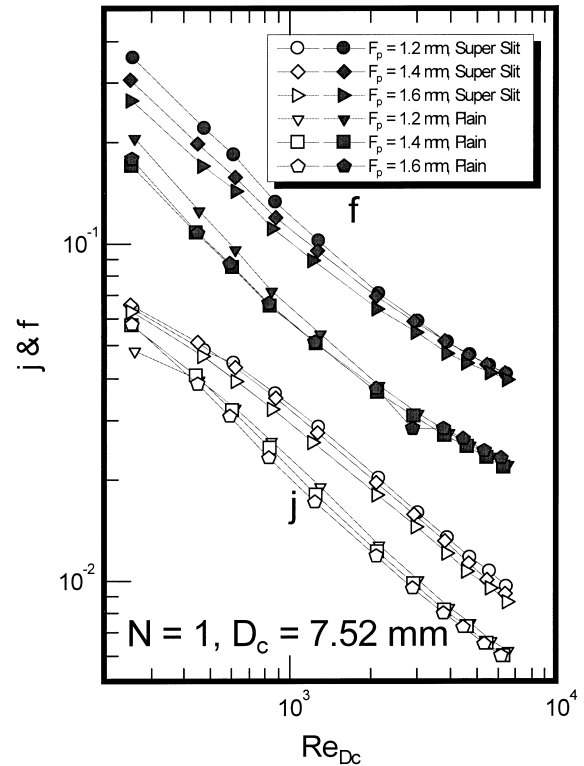


Fig. 3. Effect of fin pitch on the air side performance for type II fin geometry and  $N = 1$ .

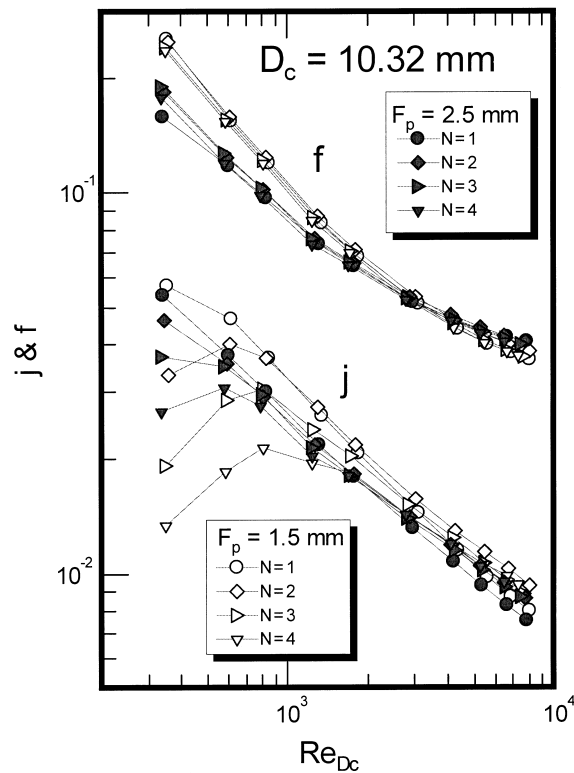


Fig. 4. Effect of the number of tube row on the air side performance for type I fin geometry.

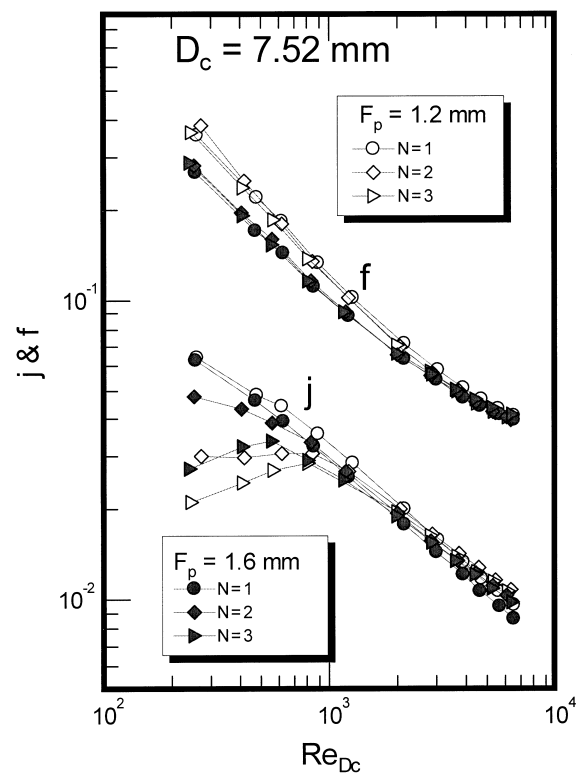


Fig. 5. Effect of the number of tube row on the air side performance for type II fin geometry.

geometry).

- The friction factors are relatively independent of the number of tube row.
- A correlation is proposed for the present slit fin configuration, the mean deviations of the proposed heat transfer and friction correlation are 8.04% and 5.44%, respectively.

#### Acknowledgements

The financial support of this work is provided by the Energy R&D foundation funding from the Energy Commission of the Ministry of Economic Affairs, Taiwan.

#### References

- [1] R.S. Mullisen, R.I. Loehrke, A study of the flow mechanisms responsible for heat transfer enhancement in

interrupted-plate heat exchangers, *ASME J. of Heat Transfer* 108 (1986) 377–385.

- [2] S. Mochizuki, Y. Yagi, W.J. Yang, Transport phenomena in stacks of interrupted parallel-plate surfaces, *Experimental Heat Transfer* 1 (1987) 127–140.
- [3] N.C. Dejong, A.M. Jacobi, An experimental study of flow and heat transfer in parallel-plate arrays: local, row-by-row and surface average behavior, *Int. J. Heat mass Transfer* 40 (1997) 1365–1378.
- [4] L.W. Zhang, S. Balachandar, D.K. Tafti, F.M. Najjar, Heat transfer enhancement mechanisms in inline and staggered parallel-plate fin heat exchangers, *Int. J. Heat mass Transfer* 40 (1997) 2307–2325.
- [5] W. Nakayama, L.P. Xu, Enhanced fins for air-cooled heat exchangers — heat transfer and friction correlations, in: *Proceeding of the 1st ASME/JSME Thermal Engineering Joint Conference* vol. 1, 1983, pp. 495–502.
- [6] C.C. Wang, W.H. Tao, C.J. Chang, An investigation of the airside performance of the slit fin-and-tube heat exchangers, *Int. J. of Refrigeration* 22 (1999) 595–603.
- [7] S. Garimella, J.W. Coleman, A. Wicht, Tube and fin geometry alternatives for the design of absorption-heat-pump heat exchangers, *J. of Enhanced Heat Transfer* 4 (1997) 217–235.
- [8] R.J. Moffat, Describing the uncertainties in experimen-

- tal results, *Experimental Thermal and Fluid Science* 1 (1988) 3–17.
- [9] C.C. Wang, C.J. Lee, C.T. Chang, Some aspects of the fin-and-tube heat exchangers: with and without louvers, *J. of Enhanced Heat Transfer* 6 (1999) 357–368.
- [10] L.L. Pauley, J.E. Hodgson, Flow visualization of convex louver fin arrays to determine maximum heat transfer conditions, *Exp. Thermal Fluid Sci.* 9 (1994) 53–60.
- [11] S. Mochizuki, Y. Yagi, W.J. Yang, Flow pattern and turbulence intensity in stacks of interrupted parallel surfaces, *Experimental Thermal and Fluid Science* 1 (1988) 51–57.